REFERENCES

[1] Z. Gu, Y. Ma, W. Yang, G. Zhang and J. Yao, *Chem. Commun.*, **28** (2005) 3597- 3599.

[2] A. Phuruangrat, D.J. Ham, S.J. Hong, S. Thongtem and J.S. Lee, *J. Mater. Chem.*, **20** (2010) 1683–1690.

[3] Z. Gu, H. Li, T. Zhai, W. Yang, Y. Xia, Y. Ma and J. Yao, *J. Solid State Chem.*, **180** (2007) 98–105.

[4] E. Zelazowska and E. Rysiakiewicz-Pasek, *J. Non-Cryst. Solids*, **354** (2008) 4500–4505.

[5] S.R. Bathe and P.S. Patil, *Solid State Ionics*, **179** (2008) 314–323.

[6] J.H. Ha, P. Muralidharan and D.K. Kim, *J. Alloys Compd.*, **475** (2009) 446–451.

[7] I.M. Szilagyi, S. Saukko, J. Mizsei, A.L. Toth, J. Madarasz and G. Pokol, *Solid Stat Sci.*, **12** (2010) 1857-1860.

[8] X. Song, Y. Zhao and Y. Zheng, *Mater. Lett.*, **60** (2006) 3405–3408.

[9] X.C. Song, Y.F. Zheng, E. Yang and Y. Wang, *Mater. Lett.*, **61** (2007) 3904–3908.

[10] R. Huirache-Acuña, F. Paraguay-Delgado, M.A. Albiter, J. Lara-Romero and R. Martínez-Sánchez, *Mater. Charact.*, **60** (2009) 932 – 937.

[11] S. Salmaoui, F. Sediri and N. Gharbi, *Polyhedron*, **29** (2010) 1771–1775.

[12] N. Shankar, M.F. Yu, S.P. Vanka and N.G. Glumac, *Mater. Lett.*, **60** (2006) 771–774.

[13] K. Zhu, H. He, S. Xie, X. Zhang, W. Zhou, S. Jin and B. Yue, *Chem. Phys. Lett.*, **377** (2003) 317-321.

[14] K.D. Lee, *Thin Solid Films,* **302** (1997) 84-88.

[15] N. Asim, S. Radiman and M.A.bin Yarmo, *Mater. Lett.,* **61** (2007) 2652–2657.

[16] R.F. Mo, G.Q. Jin and X.Y. Guo, *Mater. Lett.,* **61** (2007) 3787–3790.

[17] http://www.thefullwiki.org/Tungsten_trioxide [28 January 2011]

[18] Cui, Hai-Ning, "Preparation and characterization of optical multilayered coatings for smart windows applications, Chapter 7 Tungsten Oxide Films", University of Minho press, Portugal, 2005.

[19] Y.B. Li, Y. Bando, D. Golberg and K. Kurashima, *Chem. Phys. Lett.*, **367** (2003) 214–218.

[20] K. Byrappa and T. Adschiri, *Prog. Cryst. Growth Charact. Mater.*, **53** (2007) 117-166.

[21] T. Fujimoto, "New introduction to surface active agents", Koyoto: Sanyo Chemical Industries, 1985.

[22] Laurier L. Schramn, "Surfactants: Fundamentals and Applications in the Petroleum Industry", Chapter 1: surfactants and their solutions: basic principles", Cambridge university press, Cambridge, UK, 2000 pp.6.

[23] Z. Luo, H. Li, J. Xia, W. Zhu, J. Guo and B. Zhang, *J. Cryst. Growth*, **300** (2007) 523-529.

[24] C. O. Rangel-Yagui, A. Pessoa-Jr, and D. Blankschtein, *Braz. J. Chem. Eng.*, **21** (2004) 531 – 544.

[25] S. Rajagopal, D. Nataraj, D. Mangalaraj, Y. Djaoued, J. Robichaud and O. Y. Khyzhun, *Nanoscale Res. Lett.*, **4** (2009) 1335–1342.

[26] A. Yan, C. Xie, D. Zeng, S. Cai and M. Hu, *Mater. Res. Bull.*, **45** (2010) 1541–1547.

[27] Y. Bi, D. Li and H. Nie, *Mater. Chem. Phys.*, **123** (2010) 225–230.

[28] Y. Li, X. Su, J. Jian and J. Wang, *Ceram. Int.*, **36** (2010) 1917–1920.

[29] Powder Diffract File, JCPDS-ICDD, 12 Campus Boulevard, Newtown Square, PA, U.S.A.

[30] Z.M. Sui, X. Chen, L.Y. Wang, L.M. Xu, W.C. Zhuang, Y.C. Chai and C.J. Yang, *Physica E*, **33** (2006) 308–314.

[31] H. Kavas, Z. Durmus, M. Senel, S. Kazan, A. Baykal and M.S. Toprak, *Polyhedron*, **29** (2010) 1375–1380.

[32] G. Wang, Q. Mu, T. Chen and Y. Wang, *J. Alloys Compd.*, **493** (2010) 202–207.

[33] Y.D. Wang, S. Zhang, C.L. Ma and H.D. Li, *J. Lumin.*, **126** (2007) 661–664.

[34] A. Wolcott, T.R. Kuykendall, W. Chen, S. Chen and J.Z. Zhang, *J. Phys. Chem. B*, **110** (2006) 25288–25296.

[35] I.M. Szilágyi, J. Madarász, G. Pokol, P. Király, G. Tárkányi, S. Saukko, J. Mizsei, A.L. Tóth, A. Szabó and K. Varga-Josepovits, *Chem. Mater.*, **20** (2008) 4116–4125.

[36] J. Díaz-Reyes, R.J. Delgado-Macuil, V. Dorantes-García, A. Pérez-Benítez, J.A. Balderas-López and J.A. Ariza-Ortega, *Mater. Sci. Eng. B*, **174** (2010) 182–186.

[37] E.V. Timofeeva, G.A. Tsirlina and O.A. Petrii, *Russ. J. Electrochem.*, **39** (2003) 716–726.

[38] A. Phuruangrat, D.J. Ham, S. Thongtem and J.S. Lee, *Electrochem. Commun.*, **11** (2009) 1740–1743.

[39] Z. Jiao, X.W. Sun, J. Wang, L. Ke and H.V. Demir, *J. Phys. D: Appl. Phys.*, **43** (2010) 285501.

[40] X.M. Sun, X. Chen, Z.X. Deng and Y.D. Li, *Mater. Chem. Phys.*, **78** (2002) 99–104.

[41] T. Thongtem, S. Kaowphong and S. Thongtem, *Appl. Surf. Sci.*, **254** (2008) 7765–7769

[42] Q. Xiang, G.F. Meng, H.B. Zhao, Y. Zhang, H. Li, W.J. Ma and J.Q. Xu, *J. Phys. Chem. C*, **114** (2010) 2049–2055.

[43] J.C. Sczancoski, L.S. Cavalcante, N.L. Marana, R.O. da Silva, R.L. Tranquilin, M.R. Joya, P.S. Pizani, J.A. Varela, J.R. Sambrano, M.S. Li, E. Longo and J. Andrés, *Curr. Appl. Phys.*, **10** (2010) 614–624.

[44] J. Wang, P.S. Lee and J. Ma, *J. Cryst. Growth*, **311** (2009) 316–319.

[45] A. Rougier, F. Portemer, A. Quede and M. El Marssi, *Appl. Surf. Sci.*, **153** (1999) 1–9.

[46] http://www.sciencelab.com/msds.php?msdsId=9925359 [13 February 2011]

APPENDICES

APPENDIX A

The Joint Committee for Powder Diffraction Standards (JCPDS) [29]

1. $WO_3.0.33H_2O$, JCPDS file number 00-035-0270

Name and formula

Reference code:	00-035-0270
PDF index name:	Tungsten Oxide Hydrate
Empirical formula:	$H_{0.66}O_{3.33}W$
Chemical formula:	WO_3 .0.33H_2O

Crystallographic parameters

Crystal system:	Orthorhombic
a (?):	7.3590
b (?):	12.5130
c (?):	7.7040
Alpha (?):	90.0000
Beta (?):	90.0000
Gamma (?):	90.0000
Calculated density (g/cm^3):	6.68
Volume of cell (10^6 pm^3):	709.41
Z:	12.00
RIR:	-

Subfiles and Quality

Subfiles: Inorganic

Quality: Blank (B)

Comments

References

Primary reference: Gerand, B. et al., *J. Solid State Chem.*, **38**, 312, (1981)

Unit cell: Ibid., *J. Solid State Chem.*

Peak list

No.	h	k	l	d [A]	2Theta[deg]	I [%]
1	0	2	0	6.27000	14.114	19.0
2	1	1	1	4.90000	18.089	35.0
3	0	0	2	3.84800	23.095	40.0
4	2	0	0	3.67900	24.172	7.0
5	1	3	1	3.28100	27.157	25.0
6	2	2	0	3.15100	28.300	100.0
7	2	0	2	2.65800	33.692	7.0
8	2	2	2	2.44000	36.806	40.0
9	2	4	0	2.37900	37.785	8.0
10	0	3	3	2.17100	41.564	4.0
11	0	6	0	2.09500	43.146	4.0
12	3	3	1	2.03800	44.416	7.0
13	2	4	2	2.02800	44.647	7.0
14	0	0	4	1.92600	47.150	5.0

15	4	0	0	1.84000	49.498	14.0
16	2	6	0	1.81300	50.286	14.0
17	4	2	0	1.76500	51.753	4.0
18	3	1	3	1.75700	52.006	4.0
19	2	0	4	1.70200	53.819	9.0
20	4	0	2	1.66000	55.296	30.0
21	4	2	2	1.60500	57.363	3.0
22	4	4	0	1.58600	58.115	9.0
23	0	8	0	1.56400	59.013	4.0

Stick Pattern

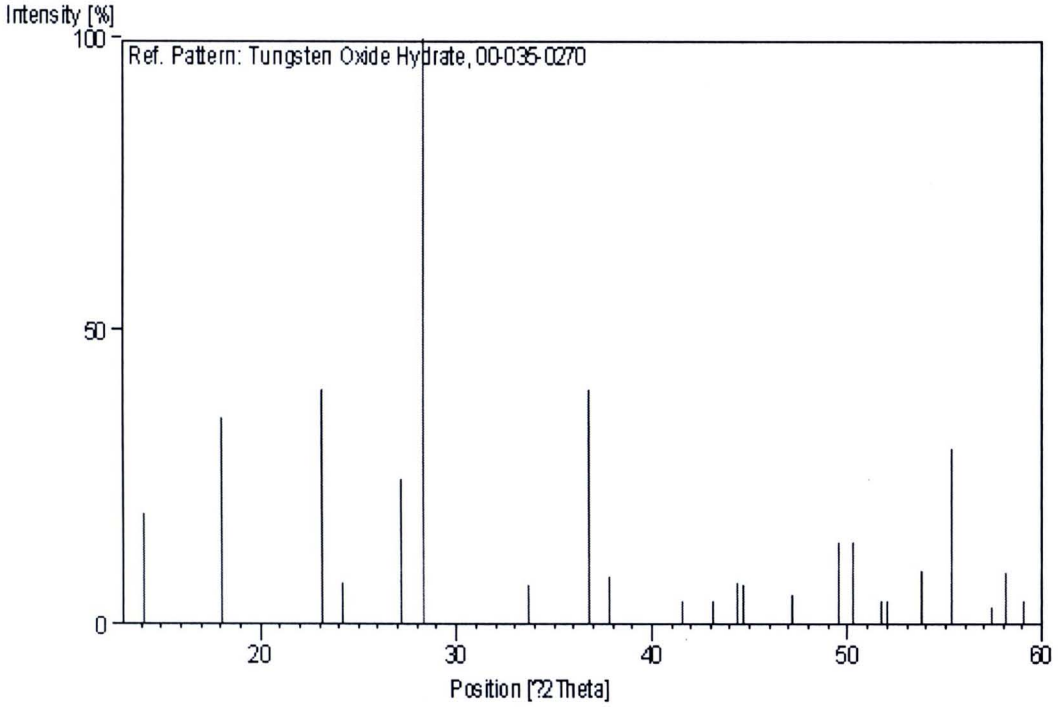

2. WO_3, JCPDS file number 00-020-1324

Name and formula

Reference code:	00-020-1324
PDF index name:	Tungsten Oxide
Empirical formula:	O_3W
Chemical formula:	WO_3

Crystallographic parameters

Crystal system:	Orthorhombic
a (?):	7.3840
b (?):	7.5120
c (?):	3.8460
Alpha (?):	90.0000
Beta (?):	90.0000
Gamma (?):	90.0000
Volume of cell (10^6 pm^3):	213.33
Z:	8.00
RIR:	-

Subfiles and Quality

Subfiles:	Inorganic
	Alloy, metal or intermetalic
	Forensic
Quality:	Indexed (I)

Comments

General comments: Stabilized with 2% Nb_2O_5.

References

Primary reference: Roth, Waring., *J. Res. Natl. Bur. Stand., Sect. A*, **70**, 281, (1966)

Peak list

No.	h	k	l	d [A]	2Theta[deg]	I [%]
1	0	0	1	3.85000	23.083	100.0
2	0	2	0	3.75000	23.707	65.0
3	2	0	0	3.69000	24.099	95.0
4	0	1	1	3.43000	25.956	2.0
5	1	2	0	3.35000	26.587	10.0
6	1	1	1	3.10000	28.776	25.0
7	0	2	1	2.68600	33.331	35.0
8	2	0	1	2.66200	33.640	35.0
9	2	2	0	2.63300	34.022	50.0
10	1	2	1	2.52500	35.525	6.0
11	2	2	1	2.17300	41.524	16.0
12	0	3	1	2.09900	43.059	2.0
13	3	2	0	2.05600	44.007	2.0
14	1	3	1	2.01800	44.880	10.0
15	3	1	1	1.99800	45.354	6.0
16	0	0	2	1.92300	47.228	20.0

17	0	4	0	1.87800	48.431	10.0
18	4	0	0	1.84600	49.326	20.0
19	1	4	0	1.82000	50.079	10.0
20	1	1	2	1.80600	50.494	16.0
21	0	2	2	1.71200	53.480	10.0
22	2	0	2	1.70600	53.683	10.0
23	0	4	1	1.68800	54.302	16.0
24	2	4	0	1.67400	54.794	10.0
25	4	0	1	1.66500	55.116	16.0
26	4	2	0	1.65700	55.404	16.0
27	1	4	1	1.64500	55.844	6.0
28	3	3	1	1.59700	57.677	2.0
29	2	2	2	1.55300	59.472	6.0
30	2	4	1	1.53500	60.242	10.0
31	4	2	1	1.52200	60.810	10.0
32	3	4	0	1.49300	62.121	6.0
33	4	3	0	1.48600	62.446	6.0

Stick Pattern

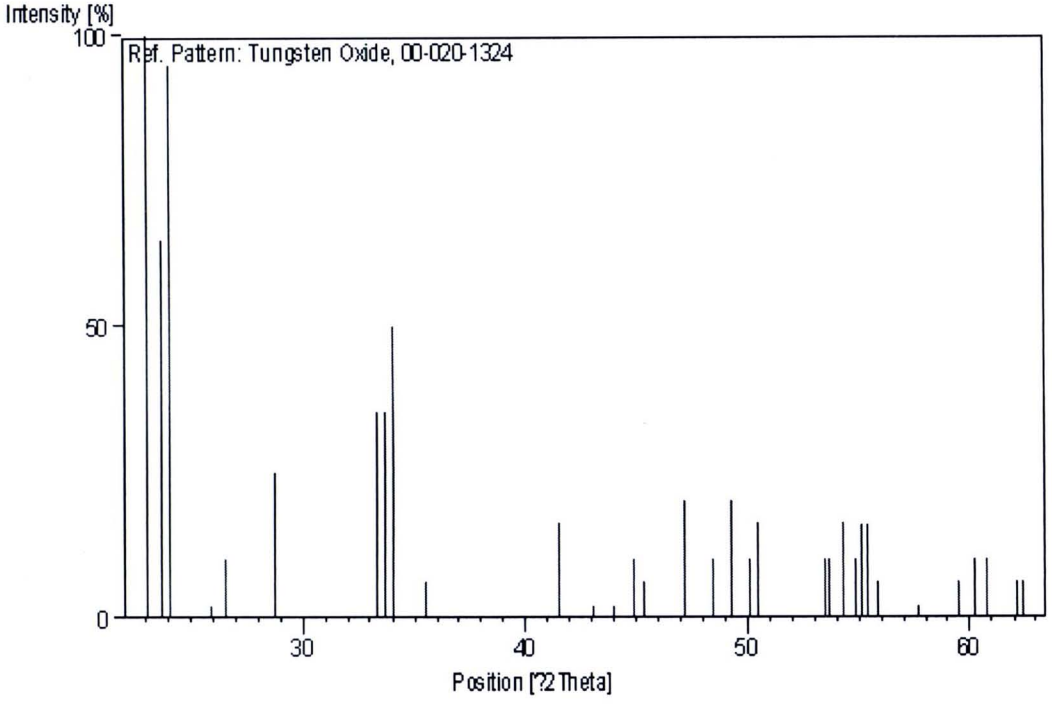

3. WO_3, JCPDS file number 00-033-1387

Name and formula

Reference code:	00-033-1387
PDF index name:	Tungsten Oxide
Empirical formula:	O_3W
Chemical formula:	WO_3

Crystallographic parameters

Crystal system:	Hexagonal
Space group:	P6/mmm
Space group number:	191
a (?):	7.2980
b (?):	7.2980
c (?):	3.8990
Alpha (?):	90.0000
Beta (?):	90.0000
Gamma (?):	120.0000
Calculated density (g/cm^3):	6.43
Measured density (g/cm^3):	6.36
Volume of cell (10^6 pm^3):	179.84
Z:	3.00
RIR:	-

Subfiles and Quality

Subfiles: Inorganic

Alloy, metal or intermetalic

Common Phase

Educational pattern

Quality: Indexed (I)

Comments

General comments: A few weak reflections on electron diffraction patterns suggested that C should be doubled for the true cell.

Sample preparation: Made by dehydration of $WO_3.0.34H_2O$ by heating at 290 C.

References

Primary reference: Gerand, B. et al., *J. Solid State Chem.*, 29, 429, (1979)

Peak list

No.	h	k	l	d [A]	2Theta[deg]	I [%]
1	1	0	0	6.34000	13.957	55.0
2	0	0	1	3.91100	22.718	50.0
3	1	1	0	3.65500	24.333	25.0
4	1	0	1	3.31800	26.848	20.0
5	2	0	0	3.16500	28.172	100.0
6	1	1	1	2.66700	33.575	9.0
7	2	0	1	2.45500	36.573	45.0
8	2	1	0	2.38800	37.637	7.0
9	3	0	0	2.10900	42.845	5.0

10	2	1	1	2.04000	44.370	4.0
11	0	0	2	1.95300	46.459	6.0
12	1	0	2	1.86400	48.818	7.0
13	3	0	1	1.85200	49.156	7.0
14	2	2	0	1.82400	49.961	20.0
15	3	1	0	1.75300	52.134	9.0
16	1	1	2	1.72100	53.178	3.0
17	2	0	2	1.65900	55.332	30.0
18	2	2	1	1.65400	55.514	30.0
19	3	1	1	1.59900	57.598	7.0
20	4	0	0	1.58100	58.316	13.0
21	2	1	2	1.51100	61.300	1.0
22	4	0	1	1.46400	63.493	10.0
23	3	2	0	1.45300	64.030	1.0
24	3	0	2	1.43000	65.186	1.0
25	4	1	0	1.37600	68.085	3.0
26	3	2	1	1.35800	69.115	1.0
27	2	2	2	1.33200	70.663	6.0
28	3	1	2	1.30300	72.481	6.0
29	1	0	3	1.27400	74.405	1.0
30	4	0	2	1.22800	77.699	4.0
31	3	3	0	1.21600	78.613	1.0
32	5	0	1	1.20000	79.870	1.0
33	4	2	0	1.19400	80.353	4.0

Stick Pattern

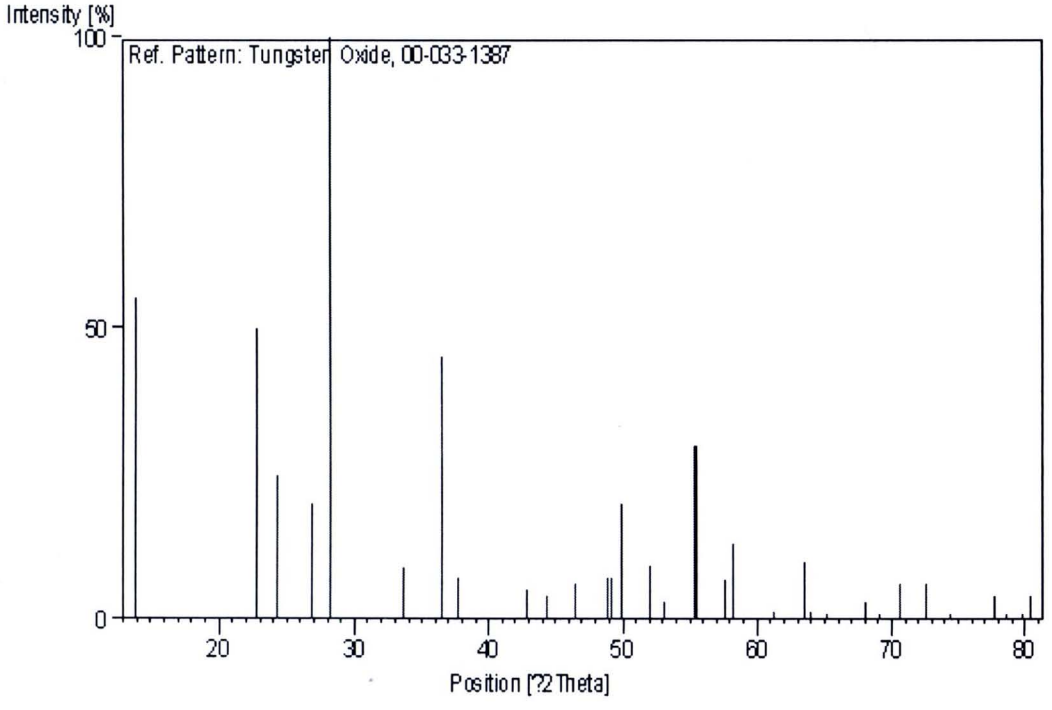

APPENDIX B

Material Safety Data Sheet [46]

ScienceLab.com
Chemicals & Laboratory Equipment

Material Safety Data Sheet
Tungsten oxide MSDS

Section 1: Chemical Product and Company Identification

Product Name: Tungsten oxide

Catalog Codes: SLT3496

CAS#: 1314-35-8

RTECS: YO7760000

TSCA: TSCA 8(b) inventory: Tungsten oxide

CI#: 77901

Synonym:

Chemical Formula: WO3

Contact Information:

Sciencelab.com, Inc.
14025 Smith Rd.
Houston, Texas 77396

US Sales: **1-800-901-7247**
International Sales: **1-281-441-4400**

Order Online: ScienceLab.com

CHEMTREC (24HR Emergency Telephone), call:
1-800-424-9300

International CHEMTREC, call: 1-703-527-3887

For non-emergency assistance, call: 1-281-441-4400

Section 2: Composition and Information on Ingredients

Composition:

Name	CAS #	% by Weight
Tungsten oxide	1314-35-8	100

Toxicological Data on Ingredients: Tungsten oxide: ORAL (LD50): Acute: 1059 mg/kg [Rat].

Section 3: Hazards Identification

Potential Acute Health Effects:
Hazardous in case of eye contact (irritant), of ingestion, of inhalation. Slightly hazardous in case of skin contact (irritant).

Potential Chronic Health Effects:
CARCINOGENIC EFFECTS: Not available. MUTAGENIC EFFECTS: Not available. TERATOGENIC EFFECTS: Not available. DEVELOPMENTAL TOXICITY: Not available. Repeated or prolonged exposure is not known to aggravate medical condition.

Section 4: First Aid Measures

Eye Contact: Check for and remove any contact lenses. Do not use an eye ointment. Seek medical attention.

Skin Contact:
After contact with skin, wash immediately with plenty of water. Gently and thoroughly wash the contaminated skin with running water and non-abrasive soap. Be particularly careful to clean folds, crevices, creases and groin. Cover the irritated skin with an emollient. If irritation persists, seek medical attention. Wash contaminated clothing before reusing.

Serious Skin Contact: Not available.

Inhalation: Allow the victim to rest in a well ventilated area. Seek immediate medical attention.

Serious Inhalation: Not available.

Ingestion:
Do not induce vomiting. Examine the lips and mouth to ascertain whether the tissues are damaged, a possible indication that the toxic material was ingested; the absence of such signs, however, is not conclusive. Loosen tight clothing such as a collar, tie, belt or waistband. If the victim is not breathing, perform mouth-to-mouth resuscitation. Seek immediate medical attention.

Serious Ingestion: Not available.

Section 5: Fire and Explosion Data

Flammability of the Product: May be combustible at high temperature.

Auto-Ignition Temperature: Not available.

Flash Points: Not available.

Flammable Limits: Not available.

Products of Combustion: Some metallic oxides.

Fire Hazards in Presence of Various Substances: Not available.

Explosion Hazards in Presence of Various Substances:
Risks of explosion of the product in presence of mechanical impact: Not available. Risks of explosion of the product in presence of static discharge: Not available.

Fire Fighting Media and Instructions:
SMALL FIRE: Use DRY chemical powder. LARGE FIRE: Use water spray, fog or foam. Do not use water jet.

Special Remarks on Fire Hazards: Not available.

Special Remarks on Explosion Hazards: Not available.

Section 6: Accidental Release Measures

Small Spill:
Use appropriate tools to put the spilled solid in a convenient waste disposal container. Finish cleaning by spreading water on the contaminated surface and dispose of according to local and regional authority requirements.

Large Spill:
Use a shovel to put the material into a convenient waste disposal container. Finish cleaning by spreading water on the contaminated surface and allow to evacuate through the sanitary system. Be careful that the product is not present at a concentration level above TLV. Check TLV on the MSDS and with local authorities.

Section 7: Handling and Storage

Precautions:
Keep away from heat. Keep away from sources of ignition. Empty containers pose a fire risk, evaporate the residue under a fume hood. Ground all equipment containing material. Do not ingest. Do not breathe dust. Avoid contact with eyes Wear suitable protective clothing In case of insufficient ventilation, wear suitable respiratory equipment If ingested, seek medical advice immediately and show the container or the label.

Storage:
Keep container dry. Keep in a cool place. Ground all equipment containing material. Keep container tightly closed. Keep in a cool, well-ventilated place. Combustible materials should be stored away from extreme heat and away from strong oxidizing agents.

Section 8: Exposure Controls/Personal Protection

Engineering Controls:
Use process enclosures, local exhaust ventilation, or other engineering controls to keep airborne levels below recommended exposure limits. If user operations generate dust, fume or mist, use ventilation to keep exposure to airborne contaminants below the exposure limit.

Personal Protection:
Splash goggles. Lab coat. Dust respirator. Be sure to use an approved/certified respirator or equivalent. Gloves.

Personal Protection in Case of a Large Spill:
Splash goggles. Full suit. Dust respirator. Boots. Gloves. A self contained breathing apparatus should be used to avoid inhalation of the product. Suggested protective clothing might not be sufficient; consult a specialist BEFORE handling this product.

Exposure Limits:
TWA: 5 STEL: 10 (mg/m3) Consult local authorities for acceptable exposure limits.

Section 9: Physical and Chemical Properties

Physical state and appearance: Solid.

Odor: Not available.

Taste: Not available.

Molecular Weight: 231.85 g/mole

Color: Not available.

pH (1% soln/water): Not applicable.

Boiling Point: Not available.

Melting Point: 1473°C (2683.4°F)

Critical Temperature: Not available.

Specific Gravity: 7.16 (Water = 1)

Vapor Pressure: Not applicable.

Vapor Density: Not available.

Volatility: Not available.

Odor Threshold: Not available.

Water/Oil Dist. Coeff.: Not available.

Ionicity (in Water): Not available.

Dispersion Properties: Not available.

Solubility: Insoluble in cold water.

Section 10: Stability and Reactivity Data

Stability: The product is stable.

Instability Temperature: Not available.

Conditions of Instability: Not available.

Incompatibility with various substances: Not available.

Corrosivity: Non-corrosive in presence of glass.

Special Remarks on Reactivity: Not available.

Special Remarks on Corrosivity: Not available.

Polymerization: No.

Section 11: Toxicological Information

Routes of Entry: Eye contact. Inhalation. Ingestion.

Toxicity to Animals: Acute oral toxicity (LD50): 1059 mg/kg [Rat].

Chronic Effects on Humans: Not available.

Other Toxic Effects on Humans:
Hazardous in case of ingestion, of inhalation. Slightly hazardous in case of skin contact (irritant).

Special Remarks on Toxicity to Animals: Not available.

Special Remarks on Chronic Effects on Humans: Not available.

Special Remarks on other Toxic Effects on Humans: Not available.

Section 12: Ecological Information

Ecotoxicity: Not available.

BOD5 and COD: Not available.

Products of Biodegradation:
Possibly hazardous short term degradation products are not likely. However, long term degradation products may arise.

Toxicity of the Products of Biodegradation: The products of degradation are as toxic as the original product.

Special Remarks on the Products of Biodegradation: Not available.

Section 13: Disposal Considerations

Waste Disposal:

Section 14: Transport Information

DOT Classification: Not a DOT controlled material (United States).

Identification: Not applicable.

Special Provisions for Transport: Not applicable.

Section 15: Other Regulatory Information

Federal and State Regulations: TSCA 8(b) inventory: Tungsten oxide

Other Regulations: Not available..

Other Classifications:

WHMIS (Canada): Not controlled under WHMIS (Canada).

DSCL (EEC):
R22- Harmful if swallowed. R36- Irritating to eyes.

HMIS (U.S.A.):

Health Hazard: 2

Fire Hazard: 1

Reactivity: 0

Personal Protection: E

National Fire Protection Association (U.S.A.):

Health: 2

Flammability: 1

Reactivity: 0

Specific hazard:

Protective Equipment:
Gloves. Lab coat. Dust respirator. Be sure to use an approved/certified respirator or equivalent. Splash goggles.

Section 16: Other Information

References: Not available.

Other Special Considerations: Not available.

Created: 10/10/2005 12:11 AM

Last Updated: 11/01/2010 12:00 PM

The information above is believed to be accurate and represents the best information currently available to us. However, we make no warranty of merchantability or any other warranty, express or implied, with respect to such information, and we assume no liability resulting from its use. Users should make their own investigations to determine the suitability of the information for their particular purposes. In no event shall ScienceLab.com be liable for any claims, losses, or damages of any third party or for lost profits or any special, indirect, incidental, consequential or exemplary damages, howsoever arising, even if ScienceLab.com has been advised of the possibility of such damages.

CURRICULUM VITAE

Name Miss Oranuch Yayapao

Date of Birth 16 July 1986

Education Background

2005 - 2008 Bachelor of Science (Chemistry),
Chiang Mai University

Scholarship

2009 - 2010 The Center of Excellence for Innovation in Chemistry
(PERCH-CIC)

Experiences

2009 Undergraduate Teaching Assistant, Chiang Mai
University, General Chemistry Laboratory

International Publication

Oranuch Yayapao, Titipun Thongtem, Anukorn Phuruangrat and Somchai Thongtem, CTAB-assisted hydrothermal synthesis of tungsten oxide microflowers, *Journal of Alloys and Compounds*, **509** (2011) 2294–2299.

Journal of Alloys and Compounds 509 (2011) 2294–2299

Contents lists available at ScienceDirect

Journal of Alloys and Compounds

journal homepage: www.elsevier.com/locate/jallcom

CTAB-assisted hydrothermal synthesis of tungsten oxide microflowers

Oranuch Yayapao [a], Titipun Thongtem [a,*], Anukorn Phuruangrat [b,*], Somchai Thongtem [c]

[a] Department of Chemistry and Center for Innovation in Chemistry, Faculty of Science, Chiang Mai University, Chiang Mai 50200, Thailand
[b] Department of Materials Science and Technology, Faculty of Science, Prince of Songkla University, Hat Yai, Songkhla 90112, Thailand
[c] Department of Physics and Materials Science, Faculty of Science, Chiang Mai University, Chiang Mai 50200, Thailand

ARTICLE INFO

Article history:
Received 6 September 2010
Received in revised form 25 October 2010
Accepted 28 October 2010
Available online 10 November 2010

Keywords:
Hydrothermal reaction
o-WO_3 microflowers
Optical properties

ABSTRACT

Orthorhombic tungsten oxide (o-WO_3) was synthesized by 200 °C, 24 h hydrothermal reactions of ammonium metatungstate hydrate solutions containing different volumes of 1 M HCl and cetyltrimethylammonium bromide (CTAB) cationic surfactant. The as-synthesized products were characterized by X-ray powder diffraction (XRD), Fourier transform infrared (FTIR) and Raman spectroscopy, and scanning and transmission electron microscopy (SEM, TEM), including UV–visible and photoluminescent (PL) spectroscopy. These analyses showed that their phases and morphologies were controlled by the acidity of the solutions. In 7.50 ml 1 M HCl-added solution, the product was o-WO_3 microflowers, with microsquare layers growing out of their cores. FTIR and Raman vibrations of W=O, O–W–O, and W–O–W stretching modes were detected, and showed typical crystalline WO_3. Their optical properties showed a maximum absorption at 275 nm in the UV region and a maximum emission peak at 375 nm. The possible formation mechanism of o-WO_3 microflowers was also proposed according the experimental results.

1. Introduction

Presently, many chemists and materials scientists are paying close attention to the study of nanostructured oxides – including zero-dimensional (0D) quantum dots, one-dimensional (1D) nanowires and nanorods, and two-dimensional (2D) nanosheets and nanodisks – because these materials have novel physical and chemical properties which are different from their corresponding bulks [1–3]. Among the different oxides with nanostructures, tungsten oxide (WO_3) has received wide attention owing to its unique photochromic and electrochromic properties. It is considered to be a promising material for multiple potential applications, including semiconductors for gas sensors, electrodes for secondary batteries, solar energy converters, and photocatalysts [3–6]. A number of synthetic methods have been developed for WO_3 such as a hydrothermal/solvothermal route [2,3,5,7], thermal processing [4], electric heating in vacuum [6], and physical/chemical vapor deposition process [8,9]. Among these, synthesis under hydrothermal conditions is a low-temperature, environmentally benign and low-cost route for preparation of nanosized oxide materials, and is becoming an increasingly attractive method [10].

In the present research, orthorhombic tungsten oxide (o-WO_3) microflowers were synthesized using a CTAB-assisted hydrothermal method. The as-synthesized o-WO_3 products were further characterized by X-ray powder diffraction (XRD), Fourier transform infrared (FTIR) and Raman spectroscopy, and scanning and transmission electron microscopy (SEM, TEM), including UV–visible (UV–vis) and photoluminescent (PL) spectroscopy.

2. Experiment

A 1.38 g of ammonium metatungstate hydrate ($(NH_4)_6H_2W_{12}O_{40}\cdot xH_2O$) was dissolved in 20 ml deionized water; 0–7.50 ml 1 M HCl was subsequently added to form H_2WO_4 with 30 min continuous stirring. CTAB surfactant (0.36 g) was added to each solution with an additional 30 min of continuous stirring. The mixtures were transferred into homemade, Teflon-lined, stainless steel autoclaves. These were tightly closed, heated at 200 °C for 24 h, and naturally cooled to room temperature. Finally, light-green precipitates were synthesized, separated by filtration, washed with deionized water and ethanol, and dried at 70 °C for 12 h.

The products were characterized and recorded on a Philips X'Pert MPD X-ray diffractometer (XRD) equipped with a graphitic monochromator of Cu Kα radiation ($\lambda = 0.1542$ nm), using a scanning rate of 0.02°/s over the 2θ range of 10–60°. FTIR spectra were recorded on PerkinElmer Spectrum RX FTIR Spectrometer with KBr as a diluting agent and operated in the range of 400–4,000 cm^{-1} with the resolution of 4 cm^{-1}. Raman vibrations of the products were detected by a HORIBA JOBIN YVON T64000 Raman spectrometer with 50 mW and 514.5 nm wavelength Ar laser. Field-emission scanning electron microscopic (FE-SEM) images were taken by a JEOL JSM-6335F operated at 15.0 kV beam energy. Transmission electron microscopic (TEM) images, and selected area electron diffraction (SAED) pattern were taken on a JEOL JEM-2010, employing at an accelerating voltage of 200 kV. UV–visible and photoluminescent spectra were carried out by a Lambda 25 spectrometer using UV lamp with the resolution of 1 nm, and LS50B Fluorescence Spectrometer, PerkinElmer, at 450 W Xe-lamp with the 0.2 nm resolution and 200 nm excitation wavelength at room temperature.

* Corresponding authors. Tel.: +66 0 53 943344; fax: +66 053 892277.
E-mail addresses: ttpthongtem@yahoo.com (T. Thongtem), phuruangrat@hotmail.com (A. Phuruangrat).

0925-8388/$ – see front matter © 2010 Elsevier B.V. All rights reserved.
doi:10.1016/j.jallcom.2010.10.204

3. Results and discussion

Fig. 1 shows the XRD patterns of the products synthesized by 200 °C, 24 h hydrothermal reactions using $(NH_4)_6H_2W_{12}O_{40}\cdot xH_2O$ and CTAB as a tungsten source and surfactant, with 0–7.50 ml 1 M HCl added. In the HCl-free solution, the product was an amorphous phase. When 2.50 ml 1 M HCl was added to the solution, both orthorhombic $WO_3\cdot 0.33H_2O$ (JCPDS No. 35-0270) and WO_3 phases (JCPDS No. 20-1324) [11] were detected. These products became pure orthorhombic WO_3 (o-WO_3) in the 5.00 ml and 7.50 ml 1 M HCl-added precursor solutions. The analysis implies that HCl has an influence on the synthesis of pure o-WO_3 phase.

SEM images (Fig. 2a and b) show o-WO_3 in the shape of ~8 μm microseeds in numerous square layers in the 5.00 ml 1 M HCl-added solution. By increasing 1 M HCl from 5.00 ml to 7.50 ml, these microsquare layers grew out of the microseed cores to form microflower-like particles (Fig. 2c and d), composed of 2–3 μm × 100–300 nm × 100–300 nm petals with very smooth surfaces.

In general, o-WO_3 has a distorted ReO_3-type structure consisting of a three-dimensional network of WO_6 octahedrons linked by their oxygen corners [5,12]. The vibrations are in the infrared (IR) range, and are classified into three regions: 600–900, 200–400 and <200 cm^{-1}, corresponding to O–W–O stretching and bending modes, and lattice vibration, respectively [13]. In this research, the products (Fig. 3) were further characterized by FTIR spectroscopy in the range of 400–4000 cm^{-1}, and the vibrations compared to those of CTAB. Some bands were detected at 2800–3020 cm^{-1}, which can be attributed to the CTAB surfactant. The FTIR spectrum of CTAB shows two intense bands at 2918 and 2846 cm^{-1}, corresponding to the asymmetric and symmetric stretching vibrations of C–CH_2 in the methylene chains. The sharp bands at 1450–1500 cm^{-1} were specified as the deformation of –CH_2– and –CH_3, and the weak band at 3011 cm^{-1} as the C–CH_3 asymmetric stretching and N–CH_3 symmetric stretching vibrations of the solid surfactant [14–17]. In case of the as-synthesized products, broad bands between 590

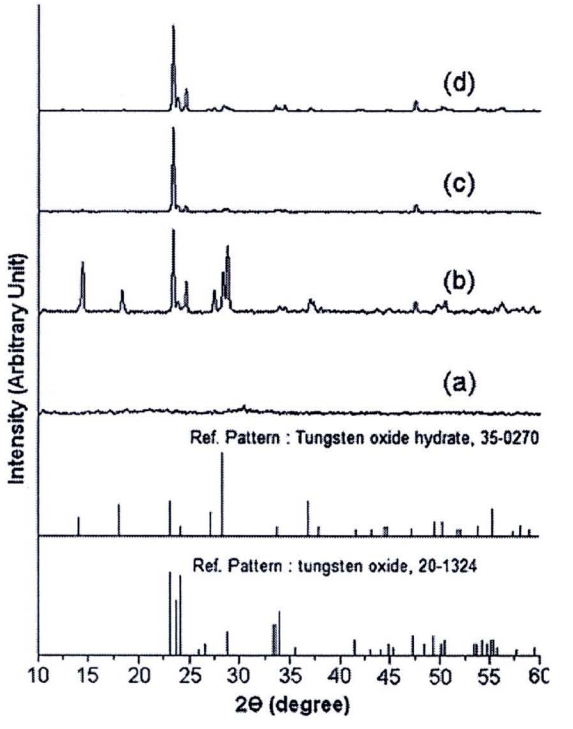

Fig. 1. XRD patterns of the products synthesized by the hydrothermal reaction at 200 °C for 24 h in the respective solutions containing (a–d) 0.00 ml, 2.50 ml, 5.00 ml, and 7.50 ml of 1 M HCl, as compared to the JCPDS standard patterns of orthorhombic $WO_3\cdot 0.33H_2O$ and WO_3 [11].

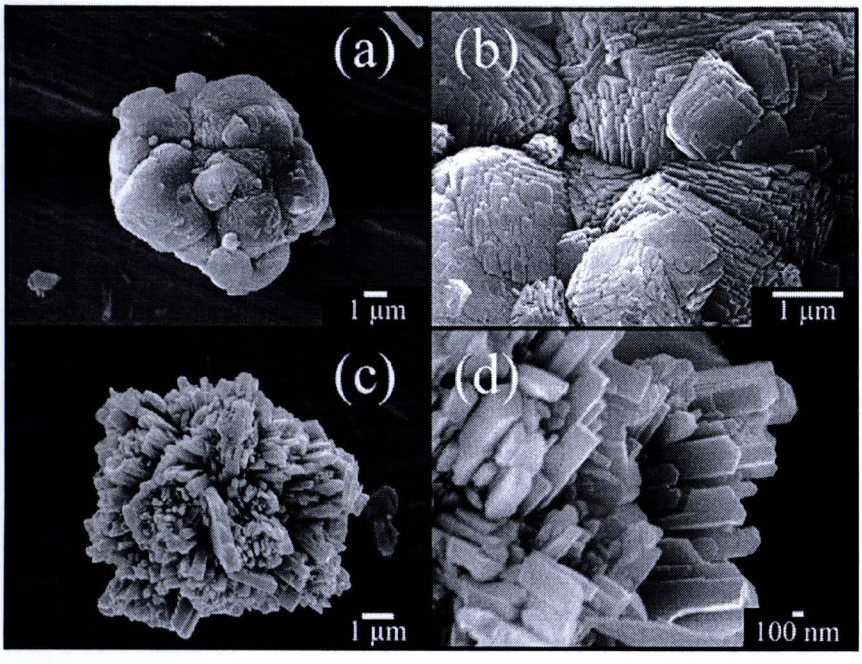

Fig. 2. SEM images of o-WO_3 synthesized by the hydrothermal reaction at 200 °C for 24 h in the solutions containing (a, b) 5.00 ml, and (c, d) 7.50 ml of 1 M HCl.

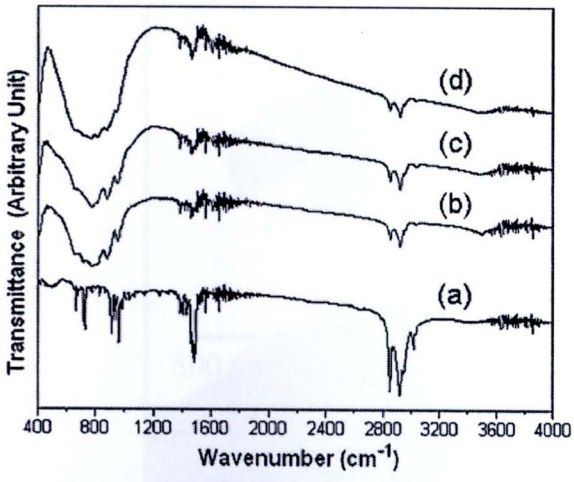

Fig. 3. FTIR spectra of (a) CTAB, and (b–d) the products synthesized by the hydrothermal reaction at 200 °C for 24 h in the solutions containing 2.50 ml, 5.00 ml, and 7.50 ml of 1 M HCl, respectively.

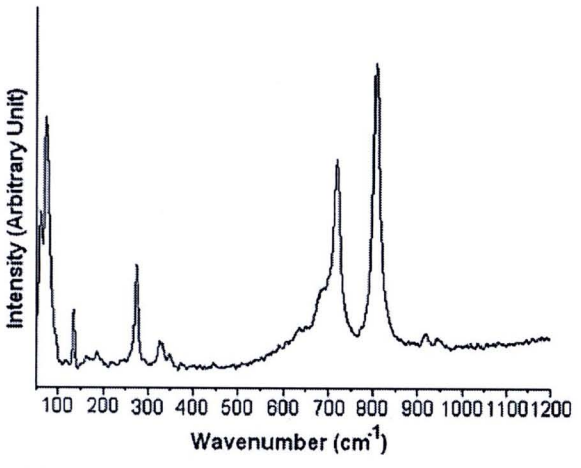

Fig. 4. Raman spectrum of o-WO_3 microflowers, synthesized by the hydrothermal reaction at 200 °C for 24 h in the solution containing 7.50 ml 1 M HCl.

and 949 cm^{-1} were detected. They are attributed to the stretching of short W=O bonds, while the bands at 817 and 728 cm^{-1} were assigned to be the O–W–O stretching modes. The vibrational bands centered at 659 and 590 cm^{-1} were attributed to the W–O–W stretching modes [5]. The asymmetric and symmetric stretching vibrations of CH_2 in the methylene chains of the incorporated CTAB were also detected at the same wavenumbers as those of the solid surfactant – implying that no intermolecular interaction was enhanced due to the capping effect, and the conformation of methylene chains remained unchanged. Their intensities are weakened, because CTAB was not completely removed by washing with deionized water and ethanol, and remained as the adsorbed head groups on the surfaces of these products – as was also found in previous reports [14,15,17].

The Raman spectrum of the as-synthesized WO_3 microflowers over the range of 50–1200 cm^{-1} is shown in Fig. 4. Generally, the 950–1050 cm^{-1} Raman wavenumbers of the transition metal oxide are assigned to be the symmetric stretching modes of metal and oxygen bonds (short terminal W=O, ν_s(W=O) terminal bands), and 750–950 cm^{-1} bands were either the antisymmetric stretching of W–O–W bonds (ν_{as}(W–O–W)) or symmetric stretching of –O–W–O– bonds (ν_s(–O–W–O–)). The Raman spectrum of the as-synthesized WO_3 microflowers detected vibrational peaks at 806, 718, 686, 326, 274, 134, 76 and 60 cm^{-1}. The two main intense peaks at 806 and 718 cm^{-1}, and the shoulder at 686 cm^{-1}, are typical Raman peaks of crystalline WO_3, which correspond to the stretching and bending vibrations of the bridging tungsten and oxygen atoms. They are assigned to be the W–O stretching (ν), W–O bending (δ) and O–W–O deformation (γ) modes, respectively. Two peaks at 326 and 274 cm^{-1} are assigned to be the bending δ(O–W–O) vibrations. Those below 200 cm^{-1} modes were attributed to the lattice vibrations. All these peaks are in good accordance with those of other reports [1,5,12,18,19].

Detailed morphology of the as-synthesized o-WO_3 structure was proved by TEM images (Fig. 5), which show the product shape to be microflowers 6–8 μm in diameter; these are composed of a large number of petals with lengths up to several micrometers. Some petals were released from the microflower cores by ultrasonic vibrations during preparation of the samples for TEM analysis. Fig. 6a and b presents high-magnification TEM images with the *x*-axis of Fig. 5b tilted. These o-WO_3 petals are straight and smooth, with uniform dimension along their axial direction. The selected area electron diffraction patterns (Fig. 6c and d) were indexed and specified as orthorhombic WO_3 phase (JCPDS No. 20-1324) [11],

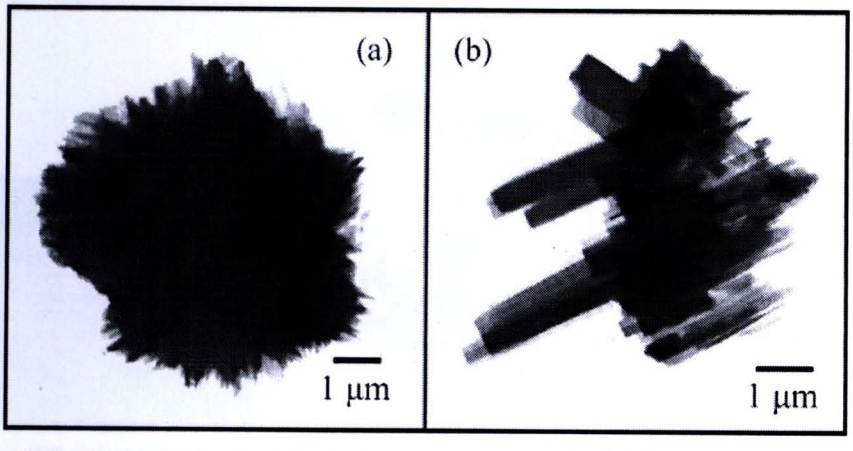

Fig. 5. TEM images of o-WO_3 microflowers, synthesized by the hydrothermal reaction at 200 °C for 24 h in the solution containing 7.50 ml 1 M HCl.

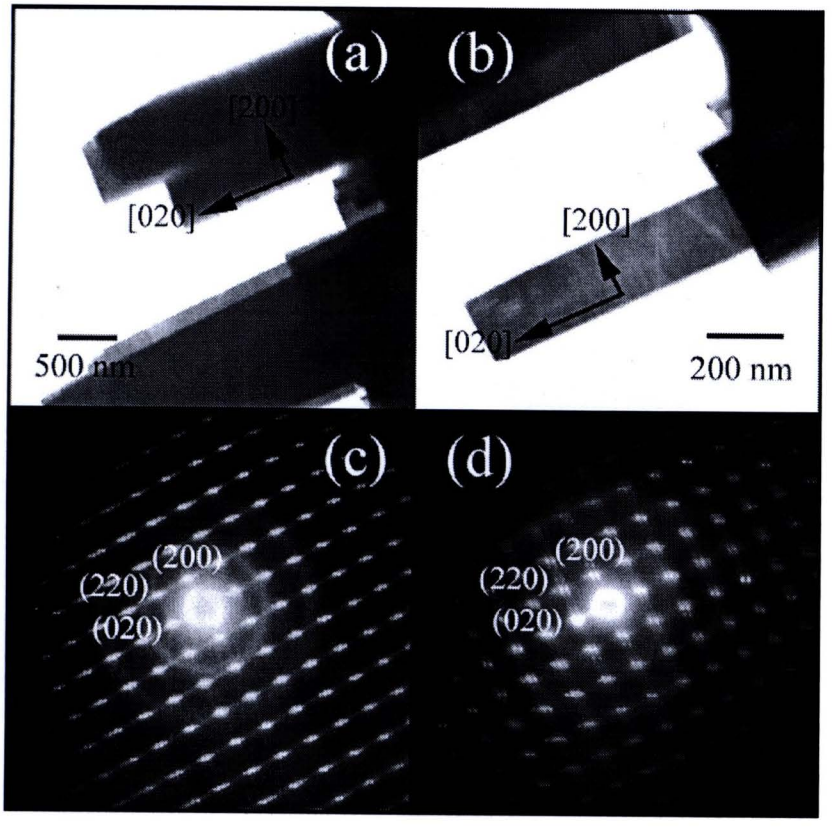

Fig. 6. (a, b) High magnification TEM images, and (c, d) SAED patterns of o-WO_3 microflowers of Fig. 5(b).

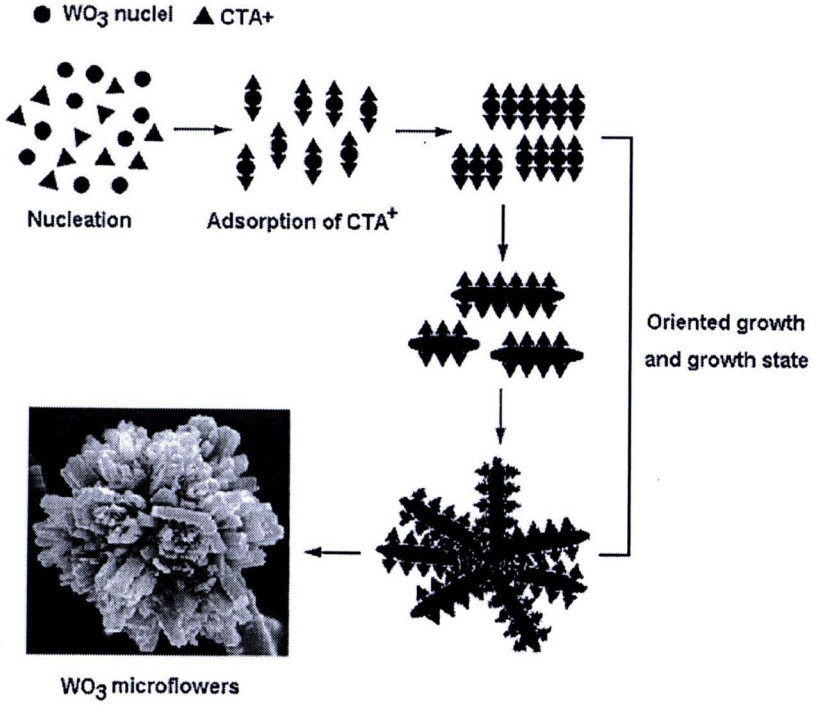

Fig. 7. Schematic diagram for the formation of o-WO_3 microflowers.

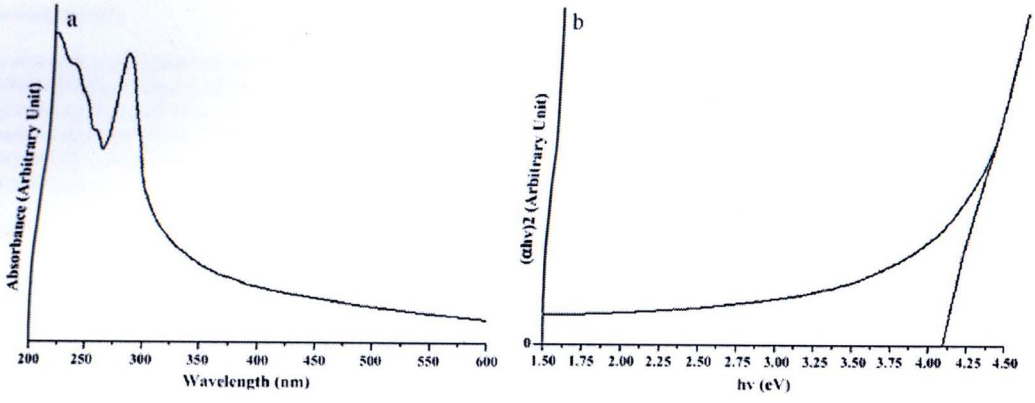

Fig. 8. (a) UV–visible spectrum, and (b) the $(\alpha h\nu)^2$ versus $h\nu$ plot of o-WO_3 microflowers, synthesized by the hydrothermal reaction at 200 °C for 24 h in the solution containing 7.50 ml 1 M HCl.

in accordance with the XRD analysis. They show the (0 2 0), (2 2 0) and (2 0 0) diffraction planes with the electron beam in the [0 0 −1] direction. It should be noted that the growth direction of the petals is normal to the (0 2 0) plane of the microsquare layers – implying that the o-WO_3 microsquare layers are aligned along the [0 2 0] direction.

The formation of o-WO_3 microflowers can be explained by polycondensation, electroneutral and dehydration reactions from the polyoxotungstate anions, as shown below:

$$H_2W_{12}O_{40}^{6-} + 6H^+ + (8+n)H_2O \rightarrow 12H_2WO_4 \cdot nH_2O \quad (1)$$

$$H_2WO_4 \cdot nH_2O \rightarrow o\text{-}WO_3(\text{nuclei}) + (n+1)H_2O \quad (2)$$

$$o\text{-}WO_3(\text{nuclei}) \rightarrow WO_3(\text{microflowers}) \quad (3)$$

When $(NH_4)_6H_2W_{12}O_{40}\cdot xH_2O$ was dissolved in deionized water, followed by the addition of HCl, the colorless solution of $H_2W_{12}O_{40}^{6-}$ anions changed to $H_2WO_4\cdot nH_2O$ yellow precursor precipitates. Upon the 200 °C hydrothermal reaction, $H_2WO_4\cdot nH_2O$ was further decomposed to produce o-WO_3 (nuclei) [20–22], containing in microsquare layers of $[WO_6]^{6-}$ octahedrons [5,12] lying in the [2 0 0] direction. At this stage, CTAB – which is a positively charged cationic surfactant (CTA^+) with a long hydrophobic tail [14,23,24] – was attracted by the four negatively charged oxygen atoms in the planar surface of $[WO_6]^{6-}$, due to the stereochemical effect. The $[CTA\text{–}WO_6]^{2-}$ bonds orientated parallel to the [0 2 0] direction inhibited growth in the [2 0 0] and [0 0 2] directions because of the CTA^+ hydrophobic tails [21,23]. The $[CTA\text{–}WO_6]^{2-}$ petals grew out from cores to form o-WO_3 microflowers, and the CTAB molecules were washed out, as shown in Fig. 7.

UV–vis absorbance for o-WO_3 microflowers (Fig. 8a) shows an absorption band in the 200–450 nm range and a strong band at 275 nm, attributed to the high UV spectrum [25]; this might be a consequence of the confined nature of electrons in the [0 1 0] direction [1]. No absorption band in the visible range was detected. This result is in accordance with those reported by Nataraj and co-workers [18], and Xu and co-workers [25]. The direct band gap (E_g) of o-WO_3 microflowers was determined by Eq. (4):

$$\alpha h\nu = (h\nu - E_g)^n \quad (4)$$

where α, h, ν, and E_g are the absorbance, Planck constant, photon frequency, and optical band gap, respectively. The parameter n is a pure number associated with the different types of electronic transitions: $n = 1/2, 2, 3/2$ or 3 for direct–allowed, indirect–allowed, direct–forbidden and indirect–forbidden transitions, respectively [26]. Its direct energy gap was determined by extrapolation of the linear portion of the curve (Fig. 8b) to $\alpha = 0$, corresponding to 4.10 eV. It should be noted that the change of absorption was controlled by two photon energy ($h\nu$) ranges – the high and low energies. When the photon energy is greater than the energy band gap (E_g), absorption was linearly increased with the increasing of photon energy. But for the photon energy with less than E_g, the absorption became different from the linearity, due to the dominant photonic absorption relating to defect levels between the valence and conduction bands of the product.

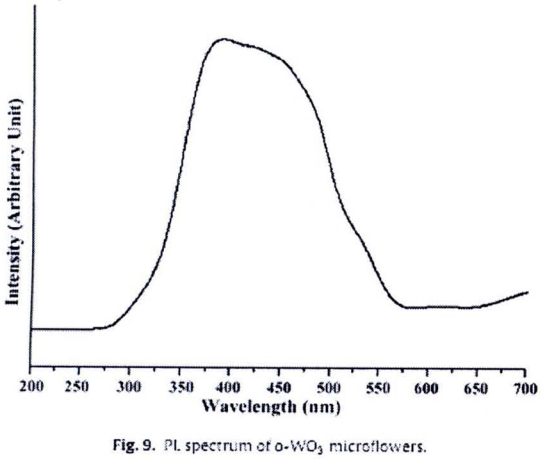

Fig. 9. PL spectrum of o-WO_3 microflowers.

The PL spectrum (Fig. 9) of the as-synthesized o-WO_3 microflowers was recorded using 200 nm excitation wavelength at room temperature. The emission peak presents a broad band at 275–575 nm with a maximum emission at 375 nm in the violet region by Gaussian curve fitting, due to the electronic transition of WO_3. This PL emission is in accordance with the report of Lee and co-workers [27].

4. Conclusions

In summary, o-WO_3 microflowers composing of long petals (E_g = 4.10 eV) were successfully synthesized by the CTAB-assisted hydrothermal reaction at 200 °C for 24 h. Their microsquare layers grew along the [0 2 0] direction to form the petals. UV spectrum shows a maximum absorption at 275 nm, and PL emission at 375 nm.

Acknowledgements

This research was supported by the National Nanotechnology Center (NANOTEC), a member of National Science and Technology Development Agency (NSTDA); Ministry of Science and Technology; Thailand Research Fund (TRF); and Center for Innovation in Chemistry (PERCH-CIC), Commission on Higher Education (CHE), Ministry of Education, Thailand.

References

[1] A. Wolcott, T.R. Kuykendall, W. Chen, S. Chen, J.Z. Zhang, J. Phys. Chem. B 110 (2006) 25288–25296.
[2] A. Yan, C. Xie, D. Zeng, S. Cai, M. Hu, Mater. Res. Bull. 45 (2010) 1541–1547.
[3] Z. Gu, Y. Ma, W. Yang, G. Zhang, J. Yao, Chem. Commun. (2005) 3597–3599.
[4] S. Sun, Y. Zhao, Y. Xia, Z. Zou, G. Min, Y. Zhu, Nanotechnology 19 (2008) 305709.
[5] S. Salmaoui, F. Sediri, N. Gharbi, Polyhedron 29 (2010) 1771–1775.
[6] D.Z. Guo, K. Yu-Zhang, A. Gloter, G.M. Zhang, Z.Q. Xue, J. Mater. Res. 19 (2004) 3665–3670.
[7] Y. Bi, D. Li, H. Nie, Mater. Chem. Phys. 123 (2010) 225–230.
[8] Y.B. Li, Y. Bando, D. Golberg, K. Kurashima, Chem. Phys. Lett. 367 (2003) 214–218.
[9] P. Tägtström, U. Jansson, Thin Solid Films 352 (1999) 107–113.
[10] Y. Li, X. Su, J. Jian, J. Wang, Ceram. Int. 36 (2010) 1917–1920.
[11] Powder Diffract File. JCPDS-ICDD, 12 Campus Boulevard, Newtown Square, PA, U.S.A.
[12] I.M. Szilágyi, J. Madarász, G. Pokol, P. Király, G. Tárkányi, S. Saukko, J. Mizsei, A.L. Tóth, A. Szabó, K. Varga-Josepovits, Chem. Mater. 20 (2008) 4116–4125.
[13] C. Guéry, C. Choquet, F. Dujeancourt, J.M. Tarascon, J.C. Lassègues, J. Solid State Electrochem. 1 (1997) 199–207.
[14] Z.M. Sui, X. Chen, L.Y. Wang, L.M. Xu, W.C. Zhuang, Y.C. Chai, C.J. Yang, Physica E 33 (2006) 308–314.
[15] H. Kavas, Z. Durmus, M. Şenel, S. Kazan, A. Baykal, M.S. Toprak, Polyhedron 29 (2010) 1375–1380.
[16] G. Wang, Q. Mu, T. Chen, Y. Wang, J. Alloys Compd. 493 (2010) 202–207.
[17] Y.D. Wang, S. Zhang, C.L. Ma, H.D. Li, J. Lumin. 126 (2007) 661–664.
[18] S. Rajagopal, D. Nataraj, D. Mangalaraj, Y. Djaoued, J. Robichaud, O.Y. Khyzhun, Nanoscale Res. Lett. 4 (2009) 1335–1342.
[19] J. Díaz-Reyes, R.J. Delgado-Macuil, V. Dorantes-García, A. Pérez-Benítez, J.A. Balderas-López, J.A. Ariza-Ortega, Mater. Sci. Eng. B 174 (2010) 182–186.
[20] E.V. Timofeeva, G.A. Tsirlina, O.A. Petrii, Russ. J. Electrochem. 39 (2003) 716–726.
[21] A. Phuruangrat, D.J. Ham, S. Thongtem, J.S. Lee, Electrochem. Commun. 11 (2009) 1740–1743.
[22] Z. Jiao, X.W. Sun, J. Wang, L. Ke, H.V. Demir, J. Phys. D: Appl. Phys. 43 (2010) 285501.
[23] X.M. Sun, X. Chen, Z.X. Deng, Y.D. Li, Mater. Chem. Phys. 78 (2002) 99–104.
[24] T. Thongtem, S. Kaowphong, S. Thongtem, Appl. Surf. Sci. 254 (2008) 7765–7769.
[25] Q. Xiang, G.F. Meng, H.B. Zhao, Y. Zhang, H. Li, W.J. Ma, J.Q. Xu, J. Phys. Chem. C 114 (2010) 2049–2055.
[26] J.C. Sczancoski, L.S. Cavalcante, N.L. Marana, R.O. da Silva, R.L. Tranquilin, M.R. Joya, P.S. Pizani, J.A. Varela, J.R. Sambrano, M.S. Li, E. Longo, J. Andrés, Curr. Appl. Phys. 10 (2010) 614–624.
[27] J. Wang, P.S. Lee, J. Ma, J. Cryst. Growth 311 (2009) 316–319.